Wavelength scanning interferometry using multiple light sources

A. Dávila*
Centro de Investigaciones en Optica
Loma del Bosque 115, Col. Lomas del Campestre
León Gto. 37150, México
*adavila@cio.mx

Abstract: A novel sensing method is proposed for wavelength scanning interferometry using multiple tunable light sources. As it is well known, a deterioration of depth resolution usually occurs when multiple phase intervals, corresponding to the multiple tunable light sources, are used for distance measurement purposes. It is shown here, that it is possible to regain depth resolution characteristics of a complete scan by means of a temporal phase unwrapping extrapolation method. With the proposed method, the resulting phase differences among multiple phase intervals can be successfully unwrapped to find out the intermediate phase. This effectively allows the application of whole-scan phase sensing for distance measurement using reduced scanning intervals, increased speed, and improved depth detection.

OCIS codes: (110.5086) Phase unwrapping; (110.4500) Optical coherence tomography; (120.5050) Phase measurement; (120.3180) Interferometry.

References and links

1. A. F. Fercher, "Optical coherence tomography: development, principles, applications," Z. Med. Phys. **20**(4), 251–276 (2010).
2. B. Heisse, *Image Processing for Phase-Sensitive Optical Coherence Tomography: Applications in Differential Phase Contrast-OCT and Polarization-Sensitive OCT Imaging.* (Suedwestdeutscher Verlag fuer Hochschulschriften, 2010).
3. P. D. Ruiz, J. M. Huntley, and R. D. Wildman, "Depth-resolved whole-field displacement measurement by wavelength-scanning electronic speckle pattern interferometry," Appl. Opt. **44**(19), 3945–3953 (2005).
4. X. Liang, V. Crecea and S. A. Boppart, "Dynamic optical coherence elastography," J. Innov. Opt. Health Sci. **3**(4), 221–233 (2010).
5. R. K. Wang, S. Kirkpatrick,and M. Hinds, "Phase-sensitive optical coherence elastography for mapping tissue microstrains in real time," Appl. Phys. Lett. **90**(16), 164105 (2007).
6. B. F. Kennedy, T. R. Hillman, R. A. McLaughlin, B. C. Quirk, and D. D. Sampson, "In vivo dynamic optical coherence elastography using a ring actuator," Opt. Express **17**(24), 21762–21772 (2009).
7. P. R. Hoskins and W. Svensson, "Current state of ultrasound elastography," Ultrasound **20**, 3–4 (2012).
8. A. Yamamoto, C. C. Kuo, and K. Sunouchi, "Surface shape measurement by wavelength scanning interferometry using an electronically tuned Ti:sapphire laser," Opt. Rev. **8**(1), 59–63 (2001).
9. A. Davila, J. M. Huntley, C. Pallikarakis, P. D. Ruiz, and J. M. Coupland, "Simultaneous wavenumber measurement and coherence detection using temporal phase unwrapping," Appl. Opt. **51**(5), 558–567 (2012).
10. A. Davila, J. M. Huntley, C. Pallikarakis, P. D. Ruiz, and J. M. Coupland, "Wavelength scanning interferometry using a Ti:Sapphire laser with wide tuning range," Opt. Laser Eng. **50**(8), 1089–1096 (2012).
11. J. Xu, Y. Liu, B. Dong, Y. Bai, L. Hu, C. Shi, Z Xu, and Y Zhou, "Improvement of the depth resolution in depth-resolved wavenumber-scanning interferometry using multiple uncorrelated wavenumber bands," Appl. Opt. **52**(20), 4890–4897 (2013).
12. C. Lu, M. Tsai, Y. Wang, Y. Kiang, and C. C. Yang, "Resolution improvement in optical coherence tomography with segmented spectrum management," Opt. Quant. Electron. **37**(13-15), 1165–1173 (2005).

#254715 Received 6 Jan 2016; revised 7 Feb 2016; accepted 11 Feb 2016; published 2 Mar 2016

13. Y. Zhang, Y. Bai, J. Xu, W. Xu and Y. Zhou, "Effective improvement of depth resolution and reduction of ripple error in depth-resolved wavenumber-scanning interferometry," Opt. Laser Eng. **66**, 58–63 (2015).
14. H. Muhamedsalih, F. Gao, and X. Jiang, "Comparison study of algorithms and accuracy in the wavelength scanning interferometry," Appl. Opt. **51**(36), 8854–8862, (2012).
15. J. M. Huntley and H. Saldner, "Temporal phase-unwrapping algorithm for automated interferogram analysis," Appl. Opt. **32**(17), 3047–3052 (1993).

1. Introduction

Wavelength scanning interferometry(WSI) and Optical Coherence Tomography (OCT) can be seen as similar techniques that differ mainly in the hardware of their optical setups, and in its signal processing approach. In particular, WSI is a volume imaging technique in which 2D image sequences are recorded as the wavenumber of the light source is tuned, ideally by linear wavenumber increments. In this technique, the intensity of the light from a given scattering point is modulated by a temporal carrier whose frequency is proportional to the optical path difference between the object and reference waves. On the other hand, OCT is a well-established technique for 3D analysis of internal structures in biological samples, and in inert materials [1, 2] that performs volume imaging by scanning consecutively 1D signals (A scans) using optical path differences over a 2D field of view. Both techniques have been, and still face many challenges to find out the best technological components for improved performance in 3D structural analysis. To overcome these challenges, the techniques developed so far can be summarized in three main categories: enhancement of depth resolution, depth range, and speed of analysis. Besides the 3D structural analysis, the OCT has also evolved to detect internal phase [2], and in WSI for phase contrast measurement [3] while in OCT and ultrasound similar techniques are known as elastography [4–6] and [7] respectively. Light sources on the other hand, are a critical component of the WSI and OCT systems, defining its overall performance. One of the main drawbacks of using the current laser technologies, is that either they have low power, or their wavelength scanning method also introduce phase noise or jitter, which limits the WSI performance. The latest technologies of tuneable lasers with high laser power are the Ti:Sapphire lasers, but still wide scan commercial ones with high resolution are hindered by mode hoping. Custom configurations have avoided mode hoping using an acousto-optic filter, and a prism with linewidths of 0.06 nm [8]. To achieve an enhanced depth of field, a mode hoping limitation of another Ti:sapphire optical configuration has been reported in [9], this was reported while trying to scan fine wavenumber steps of 0.001 nm with smaller linewidths. The mode hoping of this laser introduced multiple and undesirable mode jumps that require further processing using custom algorithms [10] to recover the depth resolution. The same limitation has been reported for broader scanning steps in semiconductor lasers, and post-processing solutions have been proposed to enhance depth resolution from multiple uncorrelated wavenumber bands [11, 12] or by reduction of ripple error [13]. As phase can be obtained either from short wavenumber scans or large wavenumber scans, the purpose of this work is to show a novel method for distance sensing of transparent materials with known refractive index, removing the depth resolution ambiguities introduced when a large wavenumber scan is divided into a series of short wavenumber scans (wavenumber bands or segments). With this approach, a direct interpolated phase is obtained that reconstructs the signal properties corresponding to a large wavenumber scan. Experimental results from a distance measurement of a glass plate confirm the validity of the proposed method.

2. Fundamentals of wavelength scanning interferometry

For a wavelength scanned interval, the interference obtained from a single layer of a material with two reflecting surfaces R and S, as represented schematically in Fig. 1(a), can be written

#254715 Received 6 Jan 2016; revised 7 Feb 2016; accepted 11 Feb 2016; published 2 Mar 2016

as:

$$I(x,y,k-\mathbf{k}) = [I_0(x,y) + I_1(x,y)\cos\{(k-\mathbf{k})\Lambda_0(x,y) + \phi_0\}]\, W[k-\mathbf{k}], \tag{1}$$

where $\mathbf{k}$ is the central wavenumber of the whole scanned interval, Λ_0 is the optical path of the layer, ϕ_0 is an initial phase shift, W is an spectral window, and the scanning is performed by sampling the wavenumber at regular time intervals t according to $k = \mathbf{k} + \delta k\, t$, in which the sampling rate is defined by the smallest wavenumber increment δk.

After obtaining the Fourier transform of Eq. (1) and removing the (x,y) dependency to simplify, we obtain

$$\tilde{I}(\Lambda) = [I_0\delta(\Lambda) + \frac{I_1}{2}\delta(\Lambda-\Lambda_0)e^{i\phi_0} + \frac{I_1}{2}\delta(\Lambda+\Lambda_0)e^{-i\phi_0}] \otimes [\tilde{W}(\Lambda)e^{-i\mathbf{k}\Lambda}]. \tag{2}$$

From this equation it can be observed that the maximum optical path range Λ_M is

$$\Lambda_M = \frac{\pi}{\delta k}, \tag{3}$$

and the optical path resolution is given by

$$\delta\Lambda = \gamma\frac{2\pi}{N_k\delta k}, \tag{4}$$

where γ is 1.207 for a rectangular window at full width half maximum, and N_k is the number of k samples. The optical path and depth distance δz, being related as usual by means of $\delta z = \Lambda_0/2\mathbf{n}$ with $\mathbf{n}$ the refractive index of the layer material.

After Fourier transform of the interference signal, the location of the peak corresponding to the single layer is shown in Fig. 1(b) and is given by $\Lambda = \Lambda_0$. Except for the constant phase terms $\mathbf{k}\Lambda_0$ and ϕ_0, the peak maxima of Eq. (2) can be used to find out an approximation to the linear phase of the cosinusoidal interference term of Eq. (1) given by the unwrapped phase $\phi_u = (k-\mathbf{k})\Lambda_0 + \phi_0$. It can be seen from this equation that for a non-dispersive layer, the phase is simply described by a linear phase change with slope Λ_0 over the whole scanning wavenumber range. In practice, the peak maximum location requires frequency interpolation with the uncertainty given by the chosen interpolation method. As N_k samples are obtained in a scan, the Fourier transform would give $N_k/2$ positive frequencies in which a given maxima can be located at a frequency that is not necessarily an integer value. The frequency corresponding to the maxima can be obtained by the derivative of the phase:

$$\nu_0 = \frac{1}{2\pi}\frac{\partial\phi}{\partial k} = \frac{\Lambda_0(x,y)}{2\pi}, \tag{5}$$

where the frequency corresponding to the maxima integer l is $\nu_0 = (l-1)/\Delta K$, with $\Delta K = N_k\delta k$, now we can calculate an approximated phase slope given by

$$\hat{\Lambda}_0(x,y) = 2\pi\frac{(l-1)}{\Delta K}. \tag{6}$$

As l can be found with floating precision using a variety of peak location methods [14], an improved accuracy is usually obtained in location and phase when efficient location methods are implemented, and when $\delta\Lambda$ is decreased by decreasing γ, and increasing N_k and δk in Eq. (4).

The corresponding wrapped phase obtained from this approximation is therefore given by:

$$\hat{\phi}_w(x,y) = k\hat{\Lambda}_0(x,y), \tag{7}$$

#254715 Received 6 Jan 2016; revised 7 Feb 2016; accepted 11 Feb 2016; published 2 Mar 2016

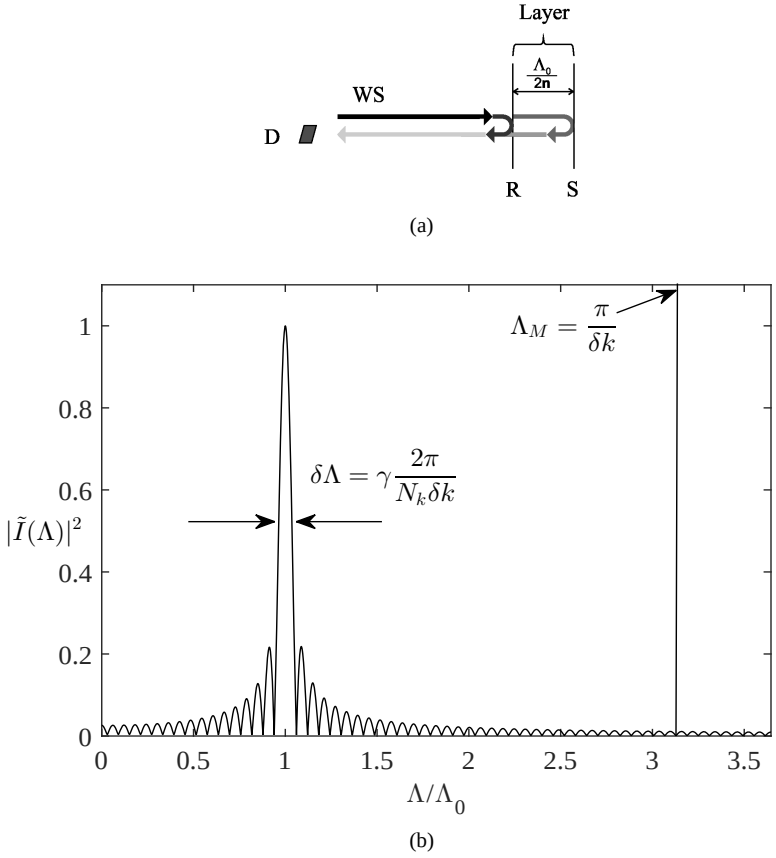

Fig. 1. (a) Schematical diagram showing a single layer material with thickness $\Lambda_0/2\mathbf{n}$, WS represents the light that is tuned at constant wavenumber rate, D is a photodetector in which the interference of two reflected beams is registered, corresponding to reflections from surfaces R and S. (b) Resolution $\delta\Lambda$ and Depth range Λ_M from the single layer of non-dispersive transparent material, obtained for the positive frequencies corresponding to the normalized power spectrum $|\tilde{I}(\Lambda)|^2$ of an interference signal acquired by detector D.

#254715 Received 6 Jan 2016; revised 7 Feb 2016; accepted 11 Feb 2016; published 2 Mar 2016

that appears wrapped, and differs from the original unwrapped phase $\phi_u = (k - \mathbf{k})\Lambda_0(x,y) + \phi_0$ in the wavenumber shift $\mathbf{k}$, and the initial phase shift ϕ_0, that are lost in the derivative process.

In the following section, the phase jumps of multiple sources with spectral gaps are first analyzed when the wavenumber bands are uniformly spaced, as a preamble to illustrate the case in which an exponential spacing method is proposed (section 4) to find out the respective phase jumps using a temporal phase unwrapping approach [15].

3. Equally spaced multi-window spectrum

To illustrate the effects on optical path resolution when multi-window spectral are considered, lets first assume that we have only two consecutive spectral windows that result from the use of two scanning light sources. If we analyze the interference pattern in WSI of the same internal structure, that for simplicity is chosen as a single layer of non-dispersing material as in Fig. 1(a). Then instead of a continuous signal we have two independent signals shown in each column of Fig. 2, where each of the two consecutive spectral WSI signals are represented in three ways: top plot as the interference signal, middle plot as the scanned phase, and bottom as the positive frequencies corresponding to the absolute value of the Fourier transform of the signal shown in the first row. As just the interference signal is only available in any measurement, the intermediate and bottom plots are usually calculated from this measurements. In any case, noise, quantization, imprecise sampling in wavenumber k, and refractive index dispersion hinders the quality of the data represented in the bottom plot, while the middle plot can also be affected by the same problems plus the phase extraction procedures.

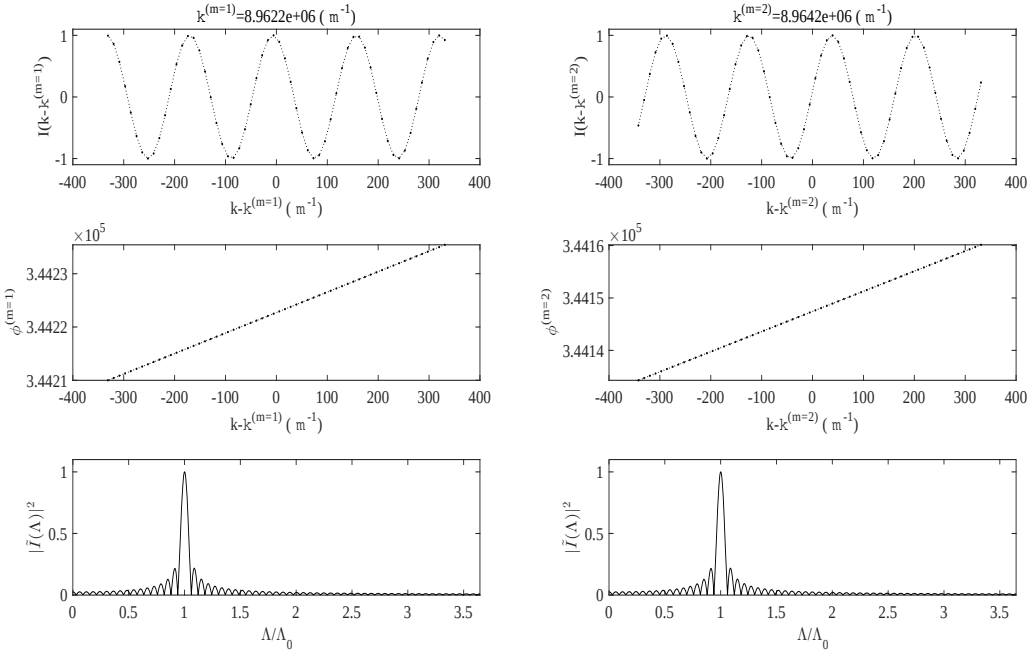

Fig. 2. Individual signals of two consecutive spectral windows shown in each column, from top to bottom: WSI normalized interference signal, unwrapped phase in radians, normalized power spectrum of interference signal shown in the first row. Samples are shown over the interpolated signal.

#254715 Received 6 Jan 2016; revised 7 Feb 2016; accepted 11 Feb 2016; published 2 Mar 2016

If we wish to obtain the phase difference among spectral windows from the intensity data, we need to implement a phase extraction procedure for each scan. A simple choice is to obtain a single phase value representing the scanned signal from the peak maxima complex value by getting the arctangent of the imaginary over the real value. However any phase difference greater than 2π among consecutive signals becomes wrapped. Another alternative is to obtain the middle plots of Fig. 2 using phase extraction methods, but the spatial unwrapping always starts from zero and the relative phase among spectral windows becomes dependent of the sampling characteristics. If sampling is well defined as a precise and constant wavenumber change, the phase jump from one spectral window to the next can be found by the number of samples that span over the void spectral band among the last sample of the first spectral window and the first sample of the second spectral window. However, experimental results using tunable light sources such as the Ti:Sapphire laser show [10] that interpolation methods are needed, as the tuning of this laser gives non-constant wavenumber increments, an example of such nonlinear increments is presented in Fig. 3.

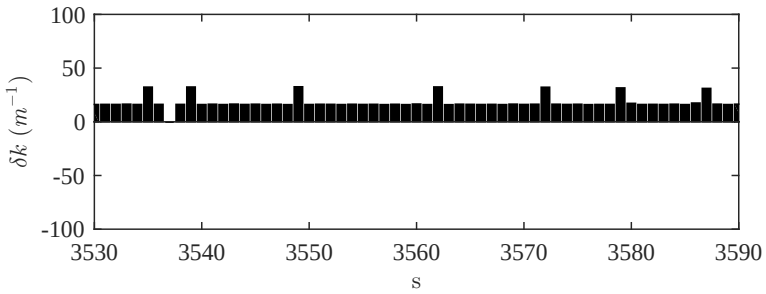

Fig. 3. Experimental wavenumber jumps δk generated by tuning a Ti:Sapphire laser in a tuning section defined by 60 samples s. The random wavenumber jumps produced by this laser cause an imprecise sampling of the interference signal, and even larger wavenumber jumps were reported [10] for larger tuning sections that required custom signal processing algorithms.

Most of the scanning methods are also frequently affected by imprecise sampling, e.g. due to time quantization of regular intervals. If imprecise sampling is considered, it might be convenient to use interpolation methods and to calculate Eq. (7) from the detected peaks of the two Fourier transforms of consecutive spectral windows, and from these to obtain the phase difference. However, as each phase is wrapped, the phase difference among the two spectral windows might have an integer number of 2π that is unknown. In any case of phase extraction, the calculated phase values that are obtained from the intensity signals are wrapped. Therefore, it is necessary to introduce a phase unwrapping algorithm to deal with the unknown number of phase jumps of 2π that exist among consecutive phases of each spectral window.

#254715 Received 6 Jan 2016; revised 7 Feb 2016; accepted 11 Feb 2016; published 2 Mar 2016

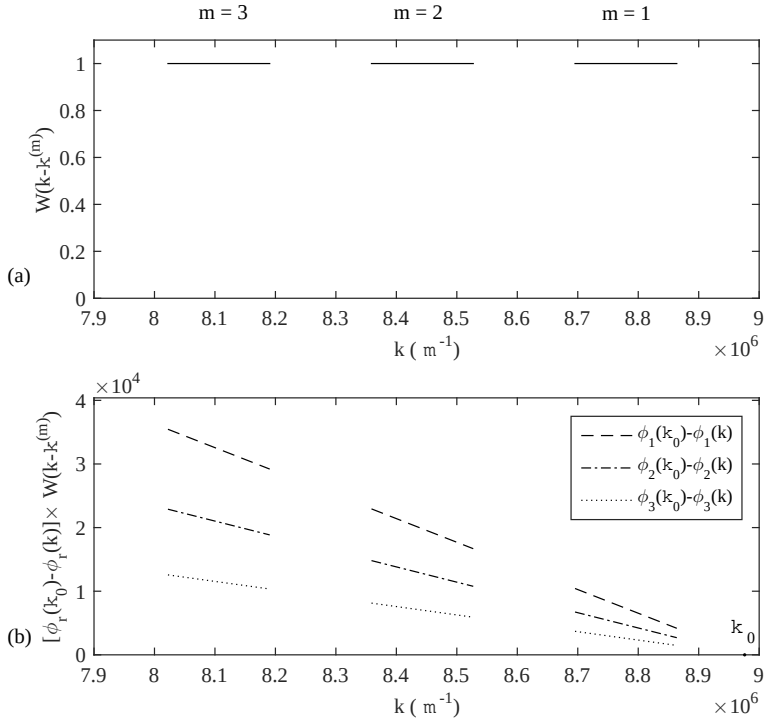

Fig. 4. Simulation of a wavelength scanning interferometer with object under inspection conformed by two layers of constant refractive index. (a) Binary spectral shaping due to multiple light sources with same spectral width and spacing in wavenumber. (b) Phase differences in radians for three peaks of a two layer object, each peak denoted consecutively by $r = 1,2,3$ with respect to the initial scanning wavenumber $\mathbf{k}_0$, notice that the spectral shaping of (a) removes phase data from a continuous or full spectral windows showing discontinuous phase data corresponding to the spectral windows $m = 1,2,3$. Each segment of a labeled line has the same slope corresponding to a peak r, as a non-dispersive refractive index was considered in this simulation.

To illustrate the multi-window spectrum in more detail, lets now assume that our object under inspection is now formed by two layers of constant refractive index. In this case, the phase term of Eq. (1) would need to be modified to include the two refractive indexes and its combination, and Eq. (2) would give three peaks on the positive frequencies of the Fourier transform, where we will indicate each peak of the Fourier transform using r as an index for each peak. Figure 4(b) shows a simulation of this process for obtaining the phase produced by interference of light from the two layers that were calculated with constant refractive indexes $n_1 = 1.452$ and $n_2 = 1.5$, with respective thickness of $d_1 = 12.8mm$ and $d_2 = 8mm$. The scanning interval was of $100nm$ with a wavelength scanning starting at $700nm$. Each peak phase can be represented schematically by the linear plots shown in Fig. 4(b) where the spectral shaping shown in Fig. 4(a) for $m = 1,2,3$ windows eliminates parts of the continuous linear phase in Fig. 4(b). Therefore, the phase of the individual line segments corresponds to a simulation of independent light sources centered at wavenumbers $\mathbf{k}^{(m)}$.

Using the discontinuous phase data from a single line of Fig. 4(b) to obtain the interfer-

#254715 Received 6 Jan 2016; revised 7 Feb 2016; accepted 11 Feb 2016; published 2 Mar 2016

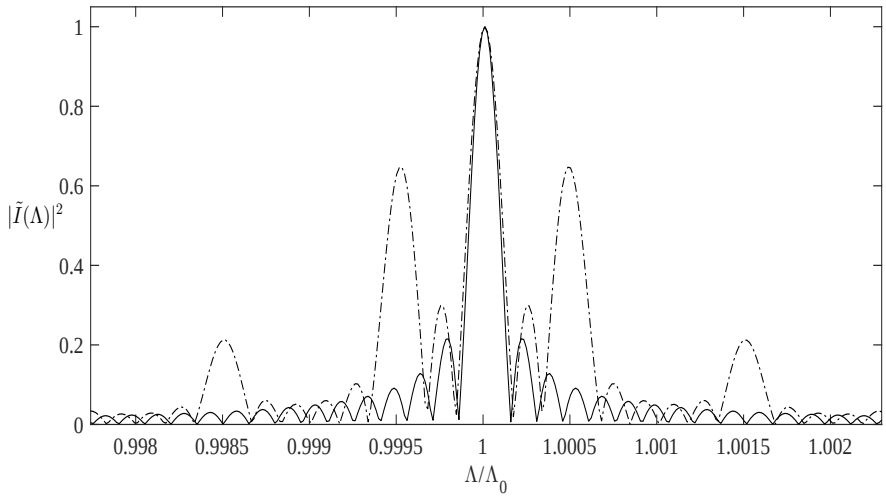

Fig. 5. Normalized power spectrum of the multiple signals shown in dash-dot line that presents higher secondary lobes compared to the continuous signal shown in continuous line. Even that the depth resolution remains the same for both signals, the secondary lobes caused by the signal disruption makes the detection of the central lobe ambiguous.

ence signal, it can be shown that the depth resolution $\delta\Lambda$ remains unaffected by the signal gaps that appear due to the multiple light sources, however the secondary lobes are magnified dis-proportionally with respect to the central peak as shown in the dotted line of Fig. 5 where constant refractive index was assumed, and both signals spanned over the same scanning interval. Therefore, peak detection in the case of multiple light sources is highly affected by the secondary maxima, that starts to compete with the main lobe for thresholds higher than 0.6 of our simulation. The peak ambiguity is even further deteriorated in the case of multiple sources when refractive index dispersion is introduced altogether with sampling uncertainty e.g. with experiments using a Ti:Sapphire tunable laser and sampling corresponding to the experimental data presented in Fig. 3.

The problems introduced by multiple sources are the main drawbacks that deter the choice of this technology, then most of the techniques available so far, prefer a whole scanning interval to obtain unambiguous depth detection and resolution represented by the solid line of Fig. 5.

Having multiple windows spaced in wavenumbers intervals can be used as a priory information to find out the phase jumps that occur among spectral windows. In particular if $\Delta\mathbf{k}_1^{(m=1,2)}$ is the known wavenumber spacing among the first two central wavenumbers of the phase ϕ_1 of Fig. 4(b), it can be used to find the simplest linear phase jump $\Delta\boldsymbol{\phi}_1^{(m=1,2)} = \Delta\mathbf{k}_1^{(m=1,2)}\Lambda_1$. In general terms we can define a phase ϕ_r, where r denotes each corresponding peak of the spectrum, with phase jumps among the first central and the Q central wavenumbers given by $\Delta\boldsymbol{\phi}_r^{(m=1,Q)} = \Delta\mathbf{k}_r^{(m=1,Q)}\Lambda_r$ that lead us to define the following equivalent constants for the whole phase of each corresponding peak r as:

$$\Lambda_r = \frac{\Delta\boldsymbol{\phi}_r^{(m=1,Q)}}{\Delta\mathbf{k}_r^{(m=1,Q)}}. \tag{8}$$

The main problem is that the phase should be unwrapped to make this equation valid. Our proposed approach uses this Eq. (8) for each phase difference to find out the best approximation

#254715 Received 6 Jan 2016; revised 7 Feb 2016; accepted 11 Feb 2016; published 2 Mar 2016

of Λ_r, and it is based on the iterative use of an exponential spaced spectral windows combined with a temporal phase unwrapping algorithm that match the phases of each spectral window with high precision.

4. Phase unwrapping of multi-window spectrums

Considering a single peak in the Fourier transform represented by $r = 1$, lets now assume that we have a phase difference among two spectral windows that is close enough -even overlapping- to produce correctly unwrapped phase difference values for each consecutive sample of the two spectral windows, as depicted in Fig. 6. With the spacing among spectral windows restricted to an unwrapped phase difference $\Delta\boldsymbol{\phi}_1^{(m=1,2)} < 2\pi$. This can be seen in the samples presented in Fig. 6: if we take the first sample and the 7^{th} sample, the wavenumber jump is the same than for the second sample and the 8^{th} sample, and so on for the each sample of the two spectral windows. In this case, $\Delta\boldsymbol{k}_1^{(m=1,2)}$ is a straightforward multiple of the sampling rate. In practice the sampling is not uniform, and the phase difference should be obtained from wavenumber averages corresponding to each spectral window to compensate the sampling uncertainties.

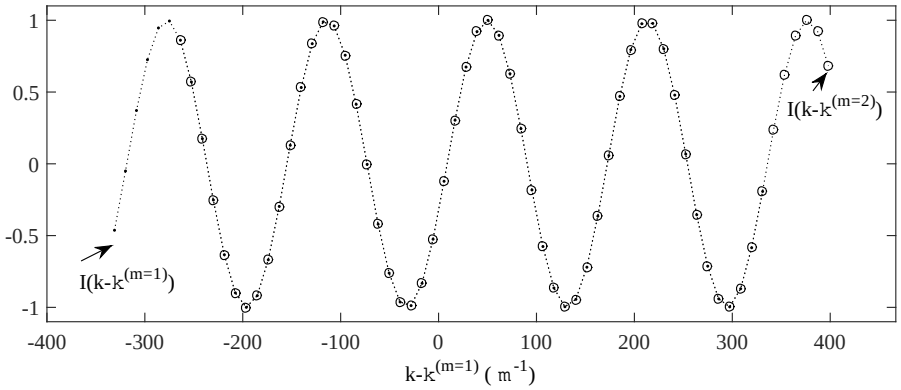

Fig. 6. Normalized interference signal with uniform sampling and two spectral windows spaced by a phase change less than 2π. The first spectral window is shown with point markers, while the second spectral window with circle markers. The refractive index is assumed constant due to the short scan.

To compare each sample of two consecutive spectral windows when the samples are not related by an uniform phase jump, an average phase difference of each pair of samples can be found through an approximated phase jump $\Delta\hat{\boldsymbol{\phi}}_u^{(m=1,2)} = \Delta\hat{\boldsymbol{k}}_1^{(m=1,2)}\Lambda_1$, where $\Delta\hat{\boldsymbol{k}}_1^{(m=1,2)} = \hat{\boldsymbol{k}}_1^{(m=1)} - \hat{\boldsymbol{k}}_1^{(m=2)}$ is calculated from the averaged central wavenumbers of each spectral window to compensate the sampling uncertainties, and the phase is denoted with the subindex u to stress the fact that the first phase difference is unwrapped.

Now the next unwrapped phase can be calculated from the initial phase by:

$$\Delta\hat{\boldsymbol{\phi}}_u^{(m=1,3)} = \Re_1\Delta\hat{\boldsymbol{\phi}}_u^{(m=1,2)}, \tag{9}$$

where $\Re_1$ is a scaling factor. The phase calculated from this equation is also unwrapped as it is a scaled version of the first unwrapped phase. However, any phase noise is also magnified by the scaling factor. To avoid the noise magnification, we can measure the wrapped phase $\Delta\hat{\boldsymbol{\phi}}_w^{(m=1,3)}$ that contains less noise, both phases should be equal except for a wrapping integer number that

#254715 Received 6 Jan 2016; revised 7 Feb 2016; accepted 11 Feb 2016; published 2 Mar 2016

can be easily determined, this is found using the temporal phase unwrapping approach [15] for each scaling. It is implemented by obtaining the integer number of 2π phase changes and using it to unwrap the wrapped phase values. If we call this process as an unwrapping operator $\mho$ we can apply it to the first phase difference, to obtain the second phase difference using the unwrapped (noisy) first phase difference and wrapped second phase difference (less noisy) phases:

$$\Delta\hat{\boldsymbol{\phi}}_u^{(m=1,3)} = \mho(\Delta\hat{\boldsymbol{\phi}}_w^{(m=1,3)}, \Re_1 \Delta\hat{\boldsymbol{\phi}}_u^{(m=1,2)}). \tag{10}$$

This unwrapped phase has lower noise levels, and can be used recursively by the following equation:

$$\Delta\hat{\boldsymbol{\phi}}_u^{(m=1,n)} = \mho(\Delta\hat{\boldsymbol{\phi}}_w^{(m=1,n)}, \Re_{n-2} \Delta\hat{\boldsymbol{\phi}}_u^{(m=1,n-1)}), \tag{11}$$

for $n = 3,4...Q$, so that the final phase difference $\Delta\hat{\boldsymbol{\phi}}_u^{(m=1,Q)}$ can be obtained at the end of the recursive process.

In general terms, the recursive process using this equation returns an unwrapped phase that is equivalent to the phase obtained from a full spectrum that covers the interval of all the multiple spectral windows. Its main difference with the phase obtained of a single spectral window is in its precision, that can be compared with the phase obtained from a full spectrum scan.

Up to now, this process as been assumed with phase differences among pairs of spectral windows scaled by arbitrary constants $\Re$. However, we can implement a design of the spectral windows positions in advance, with all the corresponding scaling constants based on an exponential scaling: $\Re_j = \Re^j$ for $j = 1,2...Q-2$. With this scaling factors, the spectrum bands become spaced with exponential increasing gaps covering within a few bands a large spectrum. It can be noticed that with this exponential scaling, two consecutive spectral windows have central wavenumber differences that are scaled by $\Re$. Alternatively, if the constants $\Re_j$ are no related by the exponential scaling, they can be adjusted by using the central wavenumbers of the consecutive spectral windows by means of:

$$\Re_j = (\boldsymbol{k}^{(m=1)} - \boldsymbol{k}^{(m=j+2)})/(\boldsymbol{k}^{(m=1)} - \boldsymbol{k}^{(m=j+1)}). \tag{12}$$

Therefore even if non-exponential exact growing factor is used, the scaling constants can be easily calculated using this last equation. Finally, the same unwrapping procedure can be used to process each phase corresponding to the Fourier peaks. However, if more peaks are considered, all their initial phase differences should also be restricted to less than 2π, such as a bandwidth for the peaks should be taken into account, given by the proper sampling of the interference patterns.

5. Experimental results

A wavelength scanning setup was built using three main components: a Ti:Sapphire laser, a glass wedge made of fused silica, and a CCD camera in an optical setup as the shown in Fig. 1(a). The laser was a CW Ti:Sapphire (M-Squared) with scanning $\delta\lambda = 0.004nm$ operating at 390mW, a scan was performed starting at 749.512 *nm*. Figure 7 shows on the left column the four intensities obtained on a a pixel camera after scanning 121 samples *s* for four spectral windows $m = 1,2,3,4$. The laser is provided with a wavelength detector that was used to monitor each wavelength step, and the respective wavelength scans are shown on the right column of Fig. 7.

Using the averaged central wavenumbers $\hat{\mathbf{k}}^{(m=1,2,3,4)}$ we can replace them for the central wavenumbers of Eq. (12) to obtain $\Re_1 = 33.0790$, and $\Re_2 = 37.2061$. Now using Eq. (11) recursively we obtain the unwrapped phase values shown in the second column of table 1 for each

#254715 Received 6 Jan 2016; revised 7 Feb 2016; accepted 11 Feb 2016; published 2 Mar 2016

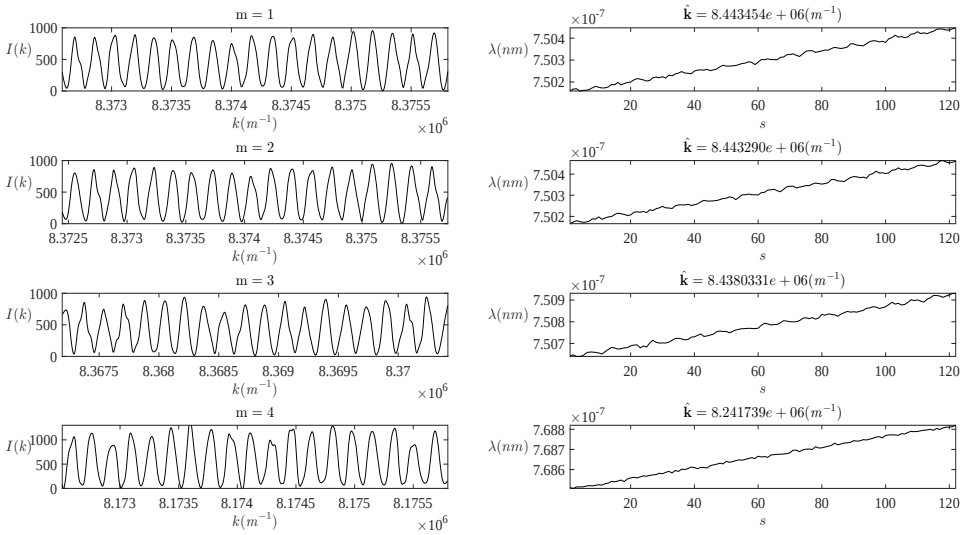

Fig. 7. From top to bottom: interference signals $I(k)$ in gray level units obtained using WSI with a glass wedge as a testing target, for four spectral bands $m = 1,2,3,4$ on the left column, with its respective wavelength scanned interval in the right column for each sample s.

pair of spectral bands $(m = 1,2)$, $(m = 1,3)$ and $(m = 1,4)$. From these values, and using the wavenumber intervals $|\Delta \boldsymbol{k}^{(m)}|$, refractive index $\mathbf{n}$ of fused silica, and Eq. (8) as the approximated optical path $\hat{\Lambda}_1$ we finally obtain the wedge thickness given by $\delta z = \hat{\Lambda}_1/2\mathbf{n}$.

Table 1. Glass wedge thickness measurement using, unwrapped phase $|\Delta \boldsymbol{\phi}_u^{(m)}|$, wavenumber intervals $|\Delta \boldsymbol{k}^{(m)}|$, and refractive index $\mathbf{n}$ for $m = 2,3,4$.

m	$\lvert\Delta \boldsymbol{\phi}_u^{(m)}\rvert$ (rad)	$\lvert\Delta \boldsymbol{k}^{(m)}\rvert$ (m^{-1})	$\mathbf{n}$	δz (mm)
$m = 1,2$	6.0519	163.8974	1.45435214465974	12.70
$m = 1,3$	200.4780	5421.5673	1.45434290787548	12.71
$m = 1,4$	7461.66044	201715.6471	1.45399832086709	12.72

The experimental measurement of the glass wedge thickness was of approximately 12.75 mm, therefore the combined measurement error of the technique, and our experimental measurement was of approximately 20 μm. However, it can seen form table 1 that the error tend to decrease when a larger number of spectral windows are considered. The obtained value of optical path resolution from Eq. (4) was of 37.5 μm and our experimental error was almost half of this value.

6. Conclusions

Phase from a whole scan has been synthesized from a series of shorts scans within spectral windows, producing an equivalent hyperspectral phase of a whole scan. As shorter spectral windows are used by the proposed technique, this technique allows an increment of processing speed for WSI. Furthermore, it has been shown in the experimental results achieved by this method, that the optical path error is even lower than the theoretical resolution obtained when a

#254715 Received 6 Jan 2016; revised 7 Feb 2016; accepted 11 Feb 2016; published 2 Mar 2016

full scan is used with standard methods, and that improved depth resolution has been achieved, overcoming the limitations caused by the shorts scans, the non-uniform sampling, and the secondary lobes caused by discontinuous intensity signals. The proposed technique can be used to extend any spectral distribution beyond the common spectral ranges of some detectors, allowing the combination of diverse detector technologies to achieve high precision measurement in WSI and OCT. The technique can also use custom spectral bands to avoid humidity spectral attenuation, or any other undesirable spectral segment that affects the measurement of a continuous spectral scan.

Acknowledgments

The experimental part of this work was developed while A. Dávila was in sabbatical year in 2008 at the Wolfson School of Mechanical and Manufacturing Engineering, Lougborough University U.K. The author would like to acknowledge all the interesting talks that took place at that time, specially with J. M. Huntley and P. D. Ruiz. Special thanks to R. Mendoza for the drawings.

#254715 Received 6 Jan 2016; revised 7 Feb 2016; accepted 11 Feb 2016; published 2 Mar 2016